Chemical composition and droplet size distribution of cloud at the summit of Mount Tai, China

Jiarong Li[1], Xinfeng Wang[1], Jianmin Chen[1,2,3,*], Chao Zhu[1], Weijun Li[1], Chengbao Li[2], Lu Liu[1], Caihong Xu[1], Liang Wen[1], Likun Xue[1], Wenxing Wang[1], Aijun Ding[3], Hartmut Herrmann[2,4,*]

[1] Environment Research Institute, School of Environmental Science and Engineering, Shandong University, Ji'nan 250100, China.

[2] Shanghai Key Laboratory of Atmospheric Particle Pollution and Prevention, Department of Environmental Science and Engineering, Institute of Atmospheric Sciences, Fudan University, Shanghai 200433, China.

[3] Institute for Climate and Global Change Research, School of Atmospheric Sciences, Nanjing University, Nanjing 210023, Jiangsu, China

[4] Leibniz Institute for Tropospheric Research (TROPOS), Atmospheric Chemistry Department (ACD), Permoserstr. 15, D-04318, Leipzig, Germany.

[*]*Correspondence to*: J. M. Chen (jmchen@sdu.edu.cn, jmchen@fudan.edu.cn); H. Herrmann (herrmann@tropos.de)

Abstract. Chemical composition of 39 cloud samples and droplet size distribution in 24 cloud events were investigated at the summit of Mt. Tai from July to October 2014. Inorganic ions, organic acids, metals, HCHO, H_2O_2, sulfur(IV), organic carbon, element carbon as well as pH and electrical conductivity were analyzed. The acidity of the cloud water significantly decreased from a reported value of pH 3.86 in 2007–2008 (Guo et al., 2012) to pH 5.87 in the present study. The concentrations of nitrate and ammonium were both increased since 2007-2008, but the overcompensation of ammonium led to the increase of the mean pH value. The microphysical properties showed that cloud droplets were smaller than 26.0 μm and the most were in the range of 6.0–9.0 μm at Mount Tai. The maximum droplet number concentration (N_d) was associated with droplet size of 7.0 μm. High LWC values could facilitate the formation of larger cloud droplets and broadened the droplet size spectra. Cloud droplets exhibited a strong interaction with atmospheric aerosols. Higher $PM_{2.5}$ level resulted in higher concentrations of water soluble ions and smaller sizes with more numbers of cloud droplets. The lower pH values were likely to occur at higher $PM_{2.5}$ concentrations. Cloud was an important sink of soluble materials in the atmosphere. The dilution effect of cloud water should be considered when estimating concentrations of soluble components in the cloud phase.

Keywords: Chemical compositions, Cloud droplet size distribution, Cloud scavenging, Mount Tai.

1 INTRODUCTION

Cloud droplets are formed by the condensation of water vapor on anthropogenic and natural aerosols that serve as cloud condensation nuclei (CCN). Clouds significantly affect the earth's radiation budget and they are also responsible for the changes in regional and global climate (Miles et al., 2000). Cloud events can transport pollutants, promote acid deposition, change the meteorological conditions, modify local environmental features and affect the fate of several atmospheric species via chemical and physical processes (Moore et al., 2004).

The chemical properties of clouds are initially determined by CCN (Sun et al., 2010). But they can be altered by absorbing chemical components of soluble gases and further multiphase chemical reactions taking place in cloud phase (Ravishankara, 1997). Non-precipitating clouds play a more crucial role in ion deposition and aggregation than precipitating clouds (Aleksic et al., 2009). The concentrations of soluble compounds and dissolved acids have generally been reported to be much higher in cloud liquid water compared with precipitation (Błaś et al., 2008; Zapletal et al., 2007; Zimmermann et al., 2003). For example, Sun and colleagues (Sun et al., 2010) found that the concentrations of ammonium, sulfate and nitrate in cloud water were at least 5.17 times higher than those in rainwater.

Cloud plays a significant role in scavenging aerosols via drop deposition (directly or by coalescence into precipitation) and in creating new particles and trace gases (Herckes et al., 2002). These processes could influence the distribution and the concentration of pollutants both in cloud phase and in aerosol phase, and also influence the microphysical properties of the clouds (Collett Jr et al., 2002; Lee et al., 2012; Ogawa et al., 2000). For example, for a given supersaturated condition, an increase in the concentration of CCN will lead to the formation of small droplets (Borys et al., 2000; Gultepe and Milbrandt, 2007). In addition, the cloud droplet size distribution (CDSD) is prominently determined by the chemical and physical properties of CCN (Portin et al., 2013; Zipori et al., 2015). Numerous studies have examined the chemical compositions of orographic clouds (Kim et al., 2006; Marinoni et al., 2004; Watanabe et al., 2010), many of which have focused on the size-dependent chemical properties of the clouds (Moore et al., 2004; Schell et al., 1997). However, few studied provide detailed descriptions of the interactions between aerosols and the chemical and microphysical properties of clouds.

In this study, cloud samples were collected at the summit of Mount Tai. It is interesting that the acidity of the cloud water was significantly lower than that reported in 2007–2008 (Guo et al., 2012; Wang et al., 2011). The causes behind this change were investigated by examining the chemical compositions of cloud samples at Mount Tai. We then investigated the microphysical properties of cloud droplets, including cloud droplet size distribution (CDSD), liquid water content (LWC), effective diameter (ED) and droplet number concentration (N_d). Lastly, we explored the interactions between cloud droplets and aerosols in the atmosphere.

2 METHODS

2.1 Site description and sampling

Mount Tai (117°13′E, 36°18′N, 1545 m a.s.l.) is a natural and cultural heritage site in China and it is one of the world's geoparks. Due to the summit of Mount Tai lacks emissions of anthropogenic pollutions, the pollutants investigated from there could accurately represent the characteristics of the regional pollutants in the North China Plain. The local high frequency of cloud events, especially in summer, makes Mount Tai a favorable site for collecting cloud samples and monitoring cloud events. Previous research has indicated that the clouds at the summit of Mount Tai are acidic (Wang et al., 2008).

From July 24 to October 31, 2014, a total of 85 cloud samples associated with 24 cloud events were collected using a single–stage Caltech Active Strand Cloud Water Collector (CASSC), as described by (Demoz et al., 1996) and 39 cloud samples were analyzed. The cloud droplets were inhaled into the collector by a fan with a flow rate of 24.5 m^3 min^{-1} and impacted on six Teflon nets that each contained 102 strands of 508 μm in diameter. The samples were then guided along a groove at the bottom of the collector and finally collected into a 500 mL high-density polyethylene cylinder. The theoretical 50% collection efficiency cut size of the cloud droplets is at 3.5 μm. In this study, sampling time resolution was adjusted during sampling sessions in order to ensure that each sample contained an adequate amount of cloud water (at least 150 mL) for the analysis. The volumes of the samples, the start and end times of the collection sessions and the numbers of collected samples were accurately recorded for each cloud event.

It should be noted that the collector was immediately shut down during precipitation to eliminate the interruptions caused by rain water. Before each sampling session, the collector was rinsed with high-purity deionized water (≥ 18.2 MΩ), dried naturally and sealed. Blanks were prepared using high-purity deionized water, and then they were treated and analyzed using the same method as collected samples.

2.2 In-situ and laboratory analysis

The pH, the electrical conductivity, the concentrations of sulfur(IV), formaldehyde, hydrogen peroxide were measured immediately after sampling. Approximately 10 mL of each cloud sample was used to measure the pH and electrical conductivity by using a portable pH meter (model 6350M, JENCO) that was regularly calibrated using standard solutions at pH =4 and pH =7. Approximately 20 mL of each cloud sample was filtered using a cellulose acetate filter with pore sizes of 0.45 μm to remove any suspended particulate matter and then the concentrations of sulfur(IV), formaldehyde and hydrogen peroxide were analyzed in-situ to avoid any changes in their concentrations. The measurement methods were described in detail by Collett and colleagues (Collett Jr et al., 1998). For each sample, a 10 mL aliquot was prepared for trace metal analysis by adding 1% (v/v) nitric acid and then preserved in a brown glass bottle at 4 ℃. Another 10 mL aliquot was prepared to analyze organic acids by adding 0.5% (v/v) chloroform (to prevent the reproduction of microorganisms) and then storing the

solution in a glass bottle at 4 ℃. The residuals were refrigerated at -20 ℃ for further analysis.

The concentrations of eight inorganic ions (Cl^-, NO_3^-, SO_4^{2-}, NH_4^+, Na^+, K^+, Ca^{2+} and Mg^{2+}) in each sample were measured using an ion-chromatography (Dionex, ICS-90) and the concentrations of four organic acids (acetate, formate, oxalate and lactate) were measured using ion-chromatography (Dionex, IC-2500) (Guo et al., 2012; Yang et al., 2012). Trace metals such as Fe and Mn were analyzed using inductively coupled plasma mass spectrometry (ICP-MS; Agilent 7500a). The concentrations of organic carbon (OC) and elemental carbon (EC) in cloud water were determined using a thermal-optical transmittance (TOT) carbon analyzer (Sunset Laboratory, Tigard, OR, USA). For each cloud sample, certain microliters were dropped on the surface of a small standard size punch (~1.5 cm^2) from a pre-combusted quartz filter and analyzed based on the NIOSH protocol 870 TOT program (Khan et al., 2009; Xu et al., 2017).

2.3 Monitoring of microphysical parameters

A fog monitor (model FM-120, Droplet Measurement Technologies Inc., USA) was used in-situ to monitor the liquid water content (LWC), the median volume diameter (MVD), the effective diameter (ED) and the droplet number concentration (N_d) of the cloud droplets with a time resolution of 1 s (DROPLET MEASUREMENT TECHNOLOGIES, 2012). During July 24 to August 23, 2014, 24 cloud events were monitored. The measuring range of cloud droplets diameter is from 2–50 μm in 20 bins. The sample velocity is 15 m s^{-1} and the sampling flow is 1 m^3 min^{-1}. Cloud droplets cannot be collected efficiently at low LWC and N_d values. Based on our experience, the sampling limitations associated with LWC and N_d were 0.01 g m^{-3} and 60 # cm^{-3}, respectively.

2.4 Measurements of ambient air pollutants and meteorological parameters

The concentrations of inorganic water–soluble ions, the levels of $PM_{2.5}$ and the meteorological parameters were monitored in real-time during the observation periods. The SO_4^{2-}, NO_3^- and NH_4^+ in $PM_{2.5}$ were measured using two on-line ion chromatographs coupled with a wet rotating denuder and a steam–jet aerosol collector (MARGA ADI 2080, Applikon-ECN). A Beta attenuation and optical analyzer (model 5030 SHARP monitor, Thermo Scientific) was used to monitor the levels of $PM_{2.5}$. Meteorological parameters including the ambient temperature, relative humidity, wind speed and wind direction were measured using an automatic meteorological station.

3 RESULTS AND DISCUSSION

3.1 Chemical properties of cloud water

3.1.1 Acidity

The pH values, electrical conductivity and chemical compositions (inorganic ions, organic acids, metals, HCHO, H_2O_2, sulfur(IV), OC, and EC) of the cloud droplets are summarized in Table 1. The pH of the cloud water varied widely from 3.80–

6.93. The volume-weighted mean (VWM) pH was 5.87, which is slightly higher than the background pH of 5.6 yielded by CO_2 in the atmosphere. The analyzed 39 cloud samples were divided into two groups. One contained 17 summer samples (i.e., those that were collected from July to August) and the other contained 22 autumn samples (i.e., those that were collected from September to October). About 52% of the summer samples was under pH of 5.6 and 12% were under pH of 4.5. The corresponding percentages for the autumn samples were 14% and 9%, respectively. It represented that some of the cloud samples at Mount Tai were acidic, especially in the summer. If comparing with other orographic stations less affected by anthropogenic pollutions, the VWM pH of clouds at Mount Tai was higher as shown in Table 2. Moreover, the VWM pH at Mount Tai significantly increased from a reported value of 3.86 in 2007–2008 (Guo et al., 2012) to 5.87 in the present study. The detailed reasons for the big decrease in cloud water acidity are discussed in the later section.

3.1.2 Chemical composition

The cloud samples contained high concentrations of water-soluble ions at Mount Tai. The dominant ions were nitrate, sulfate, ammonium and calcium by the VWM concentrations of 56.4, 44.2, 34.2 and 5.9 mg L^{-1}, respectively. These ions represented 88.1% of the total determined ion concentrations (TDIC). The concentrations of minor ions including chloride, potassium, sodium, magnesium and organic acids ranged from 0.7 mg L^{-1} to 4.1 mg L^{-1}, only amounting for 10.6% of the TDIC. Due to the frequently agricultural and livestock activities near Mount Tai, NH_4^+ was the predominant cation (Cai et al., 2015; Xu et al., 2015). Calcium was the second most abundant cation and likely originated from sandstorms and/or construction activities. The concentration of SO_4^{2-} amounted to 27.7% of the TDIC, which made SO_4^{2-} be the second most abundant anion. The concentration of non-sea salt sulfate (nss-SO_4^{2-}) was calculated using the equation [nss-SO_4^{2-}] = [SO_4^{2-}]-0.2455[Na^+]. In this equation, it assumed that the chemical properties of sea salt sulfate (ss-SO_4^{2-}) in particles are identical to those in sea water and the soluble Na^+ solely originates from sea salt (Morales et al., 1998). Through calculation, the nss-SO_4^{2-} represented 93.5–100% of the total SO_4^{2-} in this study. What's more, this might be underestimated because soil dust and biomass combustion are also sources of Na^+ besides sea salts (Lu et al., 2010; Sripa et al., 1996). The high ratio of ss-SO_4^{2-} to SO_4^{2-} indicated that anthropogenic sulfur emissions were the main sources of SO_4^{2-} in the cloud samples at Mount Tai. It should be noted that the VWM of the concentration of SO_4^{2-} was almost the same as that reported in 2007–2008, but the concentration of NO_3^- increased significantly by a factor of 2.24 (Guo et al., 2012). This made NO_3^- surpass SO_4^{2-} to be the predominant anion in 2014. The previous research indicated that the scavenging of aerosol nitrate and the uptake of gaseous nitric acid are the main sources of nitrate in cloud/fog water in generally speaking (Collett Jr et al., 2002). Our result implies that nitrate precursors (mainly NO_x from power plants and/or motor vehicles) had a substantial increase science 2007-2008.

Generally, the pH of cloud water is determined by the balance between the acid and the alkaline components. Two factors can decrease the acidity of cloud water: a large input of alkaline ions and/or a decrease in acid anions. Although the VWM concentration of NO_3^- increased significantly, the additional increases in NH_4^+ and Ca^{2+} should also be noted. Especially NH_4^+,

the VWM concentrations of NH_4^+ increased from 2007–2008 by factors of 1.56 (Guo et al., 2012). This may be attributable to the increasing consumption of agricultural fertilization and soil acidification (Cai et al., 2015; Xu et al., 2015). As a result, the increased levels of NH_4^+ and Ca^{2+} played a crucial role in neutralizing the soluble acid ions (NO_3^- and SO_4^{2-}) and decreased the acidity of cloud water in 2014.

The VWM concentrations of acetate, lactate, formate and oxalate were 4.1, 3.0, 1.75 and 0.81 mg L^{-1}, respectively, accounting for 7.01% of TDIC. Based on the sources or source strengths of formic acid and acetic acid, the formic-to-acetic acid ratio (F/A) cloud be used as an indicator to determine the sources of organic acids (Sun et al., 2016; Tan et al., 2010). Low ratio indicated the important role of direct emissions (such as biomass emission, combustion activities and aotumobile exhaust) whereas high ratio indicated the in situ photochemical generation of formic acid (Talbot et al., 1988; Tanner and Law, 2003). In the collected cloud samples, formic acid and acetic acid were highly correlated ($r=0.758$, $p \leq 0.01$). F/A was about 0.78 (lower than 1), figuring out direct emissions were important sources of organic acids (Kieber et al., 2002; Li et al., 2011). Oxalic acid was significantly correlated with formic acid ($r=0.667$, $p \leq 0.01$) and acetic acid ($r=0.638$, $p \leq 0.01$). This implied that formic acid, acetic acid and oxalic acid were probably emitted from the same sources and/or accumulated under similar physical conditions (Tanner and Law, 2003). No significant correlations were found between lactic acid and the other three carboxylic acids. No significant correlations were found between lactic acid and other water-soluble ions in the cloud samples. It implied that the emission source of lactic acid was different from formic, acetic and oxalic acids.

3.2 Microphysical properties of cloud water

3.2.1 Microphysical parameters

The sampling period, number of cloud samples, mean level of $PM_{2.5}$, mean microphysical parameters and meteorological conditions for each cloud event are summarized in Table 3. There was a great deal of diversity in the N_d and the LWC among the cloud events. The mean values of N_d ranged widely from 79 # cm^{-3} to 722 # cm^{-3} and the mean values of LWC ranged widely from 0.01 g m^{-3} to 0.39 g m^{-3}. Orographic cloud is a highly heterogeneous system consisting of randomly distributed air volumes with different characteristics (Gonser et al., 2012). This feature of orographic cloud generally determines the large differences in CDSD, LWC and aerosol composition of different cloud events.

3.2.2 Cloud droplet size distribution

The cloud droplet size distribution, which indicates the dynamic and thermodynamic properties of a cloud system, is one of the most crucial determinants of the microstructures of cloud (Yin et al., 2011). To investigate the CDSD, four typical cloud events (A, B, C and D) were studied in light of their mean $PM_{2.5}$ levels of 81.6 (A), 43.0 (B), 25.0 (C) and 11.1 μg m^{-3} (D), respectively. As shown in Fig. 1, all of the cloud droplets in cloud samples were smaller than 26.0 μm. As the cloud processes continued, droplets ranging from 6.0–9.0 μm became dominant. The ratio of cloud droplets with 6.0–9.0 μm to all droplet sizes

was relatively stable among the four cloud events (i.e., between 0.6–0.7: 1). The maximum N_d, which could reach over 1950 # m^{-3}, always occurred at a droplet size of 7.0 μm.

An examination of the meteorological parameters with the microphysical properties of the clouds showed that the LWC somewhat influenced the CDSD. Higher LWC values increased the numbers of larger cloud droplets and broadened the droplet size spectra, while lower LWC values inhibited the formation of larger cloud droplets. The formation stage of cloud event B, which occurred at 1:30–2:40 on August 23, 2014, provided a clear example. At 2:30, the LWC was relatively low with the value of 0.09 g m^{-3}. About 8.6% of the cloud droplets had diameters above 10.0 μm and 27.6% had diameters below 5.0 μm. After 8 min, the LWC sharply increased to 0.29 g m^{-3}. The corresponding ratios were 16.3% and 17.1%, respectively. Moreover, cloud droplets larger than 16.0 μm started to appear and the CDSD changed from a monomodal distribution to a weakly bimodal distribution. With the development of the cloud event, the standard deviation of CDSD represented a positive correlation with LWC values. It represented that high LWC could broaden the droplet size spectra and increase the range of cloud droplets. This situation also occurred in many other cloud events at Mount Tai.

3.2.3 Cloud scavenging effect

Cloud processes together with wet deposition play crucial roles in scavenging atmospheric aerosols. Based on the initial $PM_{2.5}$ levels, cloud processes can be classified into two types: type I (including events A and B) that have high initial $PM_{2.5}$ levels and type II (including events C and D) that have low initial $PM_{2.5}$ levels.

Type I cloud processes existed high levels of aerosol scavenging activity. Using event A as an example, at the beginning of the cloud process, there was a relatively high level of $PM_{2.5}$ (approximately 128 μg m^{-3}) and N_d increased sharply from 6 # cm^{-3} to 437 # cm^{-3} over 1 min. As the cloud process continued, the level of $PM_{2.5}$ decreased and then fluctuated with a mean concentration of 78.2 μg m^{-3}. About 30 min later, the N_d reached the maximum with 1538 # cm^{-3} and the level of $PM_{2.5}$ reached the minimum with 23.9 μg m^{-3}, which indicated a high $PM_{2.5}$ removal efficiency of 81.3%. The somewhat inverse relationship between N_d and the level of $PM_{2.5}$ reflects the efficient pollutant removal effect of cloud formation. In type II cloud processes, the levels of $PM_{2.5}$ were relatively low at the initial stage. But for both types of cloud events, the N_d significantly decreased and the $PM_{2.5}$ levels evidently increased as cloud events began to dissipate. It may due to the evaporation of water contents that condensed on the particles, which freed the CCN and formed haze. This confirmed that $PM_{2.5}$ was one of the important types of could condensation nuclei at Mt. Tai. So, $PM_{2.5}$ mass concentration was used as a proxy for CCN number concentration in this study.

3.3 Interaction between aerosols and cloud chemical properties

As illustrated in Fig. 2, the TDIC was strongly correlated with the levels of $PM_{2.5}$. High levels of $PM_{2.5}$ normally lead to high TDIC, whereas low levels of $PM_{2.5}$ usually lead to low TDIC. The pH values of cloud samples were somewhat affected by the

concentrations of $PM_{2.5}$. The lower pH values were likely to occur at higher concentrations of $PM_{2.5}$. Generally, changes of the solute concentrations in cloud water can be caused by a combination of factors such as the microphysical conditions, the CCN properties, the chemical reactions in the cloud droplets and the gas-liquid phase equilibrium (Van Pinxteren et al., 2015). Our data emphasized the crucial effect of $PM_{2.5}$ on the changes of ion concentrations. $PM_{2.5}$ are likely to be the main source of ions in cloud water.

To understand the exchange and variation of the three major ions (SO_4^{2-}, NO_3^- and NH_4^+) between the aerosol phase and the cloud phase at the summit of Mount Tai, we analyzed three cloud samples (CE-Aug23#1 from 02:30–04:38, CE-Aug23#2 from 04:38–06:21 and CE-Aug23#3 from 06:21–09:20) that were collected from the same cloud event (event B on Aug. 23, 2014). As shown in Fig. 3, in the aerosol phase, the concentrations of SO_4^{2-}, NO_3^- and NH_4^+ decreased with increases of LWC and vice versa. In the cloud phase, high LWC values meant large cloud droplets and low concentrations of major ions while low LWC values induced small cloud droplets with high levels of SO_4^{2-}, NO_3^- and NH_4^+. Elbert and colleagues also observed an inverse relationship between the ion concentrations and the LWC values (Elbert et al., 2000). Between CE-Aug23#1 and CE-Aug23#2, the ion concentrations decreased by factors of 2.29, 2.07 and 1.51 for SO_4^{2-}, NO_3^- and NH_4^+, respectively. Meanwhile, the LWC increased from 0.04 g m^{-3} to 0.32 g m^{-3} and ED increased from 6.7 μm to 10.2 μm. At the dissipation stage of the cloud event, the LWC decreased to less than 0.10 g m^{-3} and ED shrank to about 6.6 μm. Simultaneously, the ion concentrations significantly increased by factors of 1.56, 1.18 and 1.40 for SO_4^{2-}, NO_3^- and NH_4^+, respectively.

The above results demonstrate that cloud water is an important sink of soluble ions in the atmosphere and small cloud droplets tend to contain high concentrations of soluble ions than larger ones. SO_4^{2-}, NO_3^- and NH_4^+ in the aerosol phase were primarily assumed to be transferred to the cloud phase. However, the concentrations of the soluble components in the cloud phase could not be accurately predicted only based on their concentrations in the aerosol phase, as the strong dilution effect of the cloud water content must also be considered. The concentrations of ions in the cloud phase were primarily determined by two factors: the sources of the ions (i.e., the corresponding ion concentrations in the particles acted as CCN) and the LWC values (which represents the dilution effect of the cloud water). The similar variation trends of SO_4^{2-}, NO_3^- and NH_4^+ in both aerosol phase and cloud phase confirmed that LWC was an important factor affecting the ion concentrations in the cloud water at Mt. Tai (Aleksic and Dukett, 2010; Elbert et al., 2000). As mentioned above, LWC also determined the size of cloud droplets. This ultimately represented that high concentrations of soluble ions concentrated in small cloud droplets. It should be noted that, compared with SO_4^{2-} and NO_3^-, the concentration of NH_4^+ in aerosol phase did not directly increase at the dissipation stage of the cloud event. This was primarily due to the high solubility of NH_3, which dissolved in the cloud water and gave rise to the increase in the concentration of NH_4^+ in cloud sample.

3.4 Water soluble ions and droplet size under $PM_{2.5}$

Secondary inorganic compounds especially ammonium sulfate and ammonium nitrate were the main hygroscopic compounds

of particulate matters. The presence of these compounds could enhance the hygroscopic ability of atmospheric particles and facilitate their ability to act as cloud condensation nuclei (Wang et al., 2014; Ye et al., 2011). These water soluble ions are primarily transferred to the cloud phase during the formation of cloud droplets by activation of CCN. As mentioned before, SO_4^{2-}, NO_3^-, NH_4^+ and Ca^{2+} were the most predominant ions in cloud samples collected at Mount Tai. The averaged concentrations surpassed 88.1% of the total determined ion concentrations. Presumably, $PM_{2.5}$ was the main source of the mentioned soluble ions in cloud water. In order to investigate the variation trend between water soluble ions and cloud droplet size under different $PM_{2.5}$ levels, 17 cloud samples collected from 25 July to 23 August were studied as shown in Fig. 4. As can be seen, high $PM_{2.5}$ level represented high ion concentrations and small cloud droplets. It confirmed again that $PM_{2.5}$ acted as CCN was the main source of soluble ions in cloud water. High $PM_{2.5}$ levels would lead to a large source of CCN, increase the competition of ambient water vapor and hinder the formation of large cloud droplets.

It should be noticed that sometimes the N_d varied at the same $PM_{2.5}$ level in Fig. 4b. It was caused by the variation of LWC values or ambient RH in different monitoring moments (Ackerman et al., 2004). The low RH (representing there was no sufficient water vapor in the atmosphere) would impede the hygroscopic growth of particles and the activation of droplets (Gonser et al., 2012; Liu et al., 2011), affecting the formation of cloud droplets.

4 Conclusions

In 2014, samples of clouds at Mount Tai showed that the VWM pH of the cloud samples was 5.87. It is much higher than that reported by previous studies taking place at the same site in 2007–2008. The cloud water contained much higher concentrations of ions than the samples collected at other orographic sites, indicating the strong influence of anthropogenic emissions on clouds at the summit of Mount Tai. The dominant ion species were NH_4^+, SO_4^{2-}, Ca^{2+} and NO_3^-, which amounted to more than 88.1% of the TDIC. The NO_3^- content of the cloud water was significantly higher than that in 2007–2008. However, the increase of the NH_4^+ concentration (mainly from NH_3) exceeded that of NO_3^- (mainly from NO_x), leading to net neutralization and reduced the cloud acidity. The rapid increases in the concentrations of NH_4^+ and Ca^{2+} should be attributable to the agricultural fertilization and the soil acidification frequently occurred recent years (Cai et al., 2015; Xu et al., 2015). The microphysical parameters of the cloud samples varied enormously between the cloud events. The cloud droplets were all smaller than 26.0 μm and most were 6.0–9.0 μm. The maximum N_d was associated with droplet sizes of 7.0 μm. Higher LWC values could facilitate the formation of larger cloud droplets and broadened the droplet size spectra. A strong interaction was observed between the concentrations of soluble ions in cloud droplets and the levels of $PM_{2.5}$ in the atmosphere. The clouds played a crucial role in scavenging atmospheric aerosols. Higher $PM_{2.5}$ level resulted in higher TDIC. The lower pH values were likely to occur at higher $PM_{2.5}$ concentrations. We found that the dilution effect of cloud water was strong and it should not be ignored when estimating concentrations of soluble components in the cloud phase.

In summary, the mechanism of cloud droplet formation is summarized in Fig. 5. According to the concentrations of $PM_{2.5}$, cloud events were divided into two categories. One was the $PM_{2.5}$ concentrations greater than 35 μg m^{-3}. The other was the $PM_{2.5}$ concentrations less than or equal to 35 μg m^{-3}. Cloud droplets would be formed on condensation nuclei (usually aerosols including secondary aerosol, dust, sea salt, and so on) through water vapor condensation and then undergo hygroscopic growth. The soluble ions in condensation nuclei and ambient gases could enter cloud droplets through surface reactions and consequently participate dissolution, diffusion, dilution and aqueous reaction in the cloud phase. Higher aerosol concentrations supplied higher concentrations of soluble ions for cloud droplets and facilitate the formation of smaller sizes of cloud droplets, which caused the high concentrations of soluble ions in small cloud droplets.

ACKNOWLEDGEMENTS

This work was supported by Taishan Scholar Grant (ts20120552), National Natural Science Foundation of China (41375126, 41275123, 21190053, 21177025), Cyrus Tang Foundation (No. CTF-FD2014001), Ministry of Science and Technology of China (2016YFC0202701, 2014BAC22B01), Strategic Priority Research Program of the Chinese Academy of Sciences (Grant No. XDB05010200), and Natural Science Foundation of Shandong Province (No. ZR2014BQ031).

REFERENCES

Ackerman, A.S., Kirkpatrick, M.P., Stevens, D.E., Toon, O.B. (2004) The impact of humidity above stratiform clouds on indirect aerosol climate forcing. Nature 432, 1014.

Aleksic, N., Dukett, J.E. (2010) Probabilistic relationship between liquid water content and ion concentrations in cloud water. Atmos. Res. 98, 400-405.

Aleksic, N., Roy, K., Sistla, G., Dukett, J., Houck, N., Casson, P. (2009) Analysis of cloud and precipitation chemistry at Whiteface Mountain, NY. Atmos. Environ. 43, 2709-2716.

Błaś, M., Polkowska, Ż., Sobik, M., Klimaszewska, K., Nowiński, K., Namieśnik, J. (2010) Fog water chemical composition in different geographic regions of Poland. Atmos. Res. 95, 455-469.

Błaś, M., Sobik, M., Twarowski, R. (2008) Changes of cloud water chemical composition in the Western Sudety Mountains, Poland. Atmos. Res. 87, 224-231.

Borys, R.D., Lowenthal, D.H., Mitchell, D.L. (2000) The relationships among cloud microphysics, chemistry, and precipitation rate in cold mountain clouds. Atmos. Environ. 34, 2593-2602.

Budhavant, K.B., Rao, P.S.P., Safai, P.D., Granat, L., Rodhe, H. (2014) Chemical composition of the inorganic fraction of cloud-water at a high altitude station in West India. Atmos. Environ. 88, 59-65.

Cai, Z., Wang, B., Xu, M., Zhang, H., He, X., Zhang, L., Gao, S. (2015) Intensified soil acidification from chemical N fertilization and prevention by manure in an 18-year field experiment in the red soil of southern China. J. Soils Sediments 15, 260-270.

Collett Jr, J.L., Bator, A., Sherman, D.E., Moore, K.F., Hoag, K.J., Demoz, B.B., Rao, X., Reilly, J.E. (2002) The chemical composition of fogs and intercepted clouds in the United States. Atmos. Res. 64, 29-40.

Collett Jr, J.L., Hoag, K.J., Sherman, D.E., Bator, A., Richards, L.W. (1998) Spatial and temporal variations in San Joaquin Valley fog chemistry. Atmos. Environ. 33, 129-140.

Demoz, B.B., Collett Jr, J.L., Daube Jr, B.C. (1996) On the Caltech Active Strand Cloudwater Collectors. Atmos. Res. 41, 47-62.

DROPLET MEASUREMENT TECHNOLOGIES, I. (2012) Particle Analysis and Display System (PADS) 3.6.3 Overview Manual DOC-0300, Rev C-11.

Elbert, W., Hoffmann, M.R., Krämer, M., Schmitt, G., Andreae, M.O. (2000) Control of solute concentrations in cloud and fog water by liquid water content. Atmos. Environ. 34, 1109-1122.

Gonser, S.G., Klemm, O., Griessbaum, F., Chang, S.C., Chu, H.S., Hsia, Y.J. (2012) The Relation Between Humidity and Liquid Water Content in Fog: An Experimental Approach. Pure Appl. Geophys. 169, 1-13.

Gultepe, I., Milbrandt, J.A. (2007) Microphysical Observations and Mesoscale Model Simulation of a Warm Fog Case during FRAM Project. Pure Appl. Geophys. 164, 1161-1178.

Guo, J., Wang, Y., Shen, X., Wang, Z., Lee, T., Wang, X., Li, P., Sun, M., Collett Jr, J.L., Wang, W., Wang, T. (2012) Characterization of cloud water chemistry at Mount Tai, China: Seasonal variation, anthropogenic impact, and cloud processing. Atmos. Environ. 60, 467-476.

Herckes, P., Lee, T., Trenary, L., Kang, G., Chang, H., Jr, C.J. (2002) Organic matter in central California radiation fogs. Environ. Sci. Technol. 36, 4777-4782.

Khan, A.J., Swami, K., Ahmed, T., Bari, A., Shareef, A., Husain, L. (2009) Determination of elemental carbon in lake sediments using a thermal–optical transmittance (TOT) method. Atmos. Environ. 43, 5989-5995.

Kieber, R.J., Peake, B., Willey, J.D., Avery, G.B. (2002) Dissolved organic carbon and organic acids in coastal New Zealand rainwater. Atmos. Environ. 36, 3557-3563.

Kim, M.-G., Lee, B.-K., Kim, H.-J. (2006) Cloud/Fog Water Chemistry at a High Elevation Site in South Korea. J. Atmos. Chem. 55, 13-29.

Lee, A.K.Y., Hayden, K.L., Herckes, P., Leaitch, W.R., Liggio, J., Macdonald, A.M., Abbatt, J.P.D. (2012) Characterization of aerosol and cloud water at a mountain site during WACS 2010: secondary organic aerosol formation through oxidative cloud processing. Atmos. Chem. Phys. Discuss. 12, 7103-7116.

Li, P., Li, X., Yang, C., Wang, X., Chen, J., Collett Jr, J.L. (2011) Fog water chemistry in Shanghai. Atmos. Environ. 45, 4034-4041.

Liu, P.F., Zhao, C.S., Bel, T.G., Hallbauer, E., Nowak, A., Ran, L., Xu, W.Y., Deng, Z.Z., Ma, N., Mildenberger, K. (2011) Hygroscopic properties of aerosol particles at high relative humidity and their diurnal variations in the North China Plain. Atmos. Chem. Phys. 11, 3479-3494.

Lu, C., Niu, S., Tang, L., Lv, J., Zhao, L., Zhu, B. (2010) Chemical composition of fog water in Nanjing area of China and its related fog microphysics. Atmos. Res. 97, 47-69.

Marinoni, A., Laj, P., Sellegri, K., Mailhot, G. (2004) Cloud chemistry at the Puy de Dôme: variability and relationships with environmental factors. Atmos. Chem. Phys. 4, 715-728.

Michna, P., Werner, R.A., Eugster, W. (2015) Does fog chemistry in Switzerland change with altitude? Atmos. Res. 151, 31-44.

Miles, N.L., Verlinde, J., Clothiaux, E.E. (2000) Cloud Droplet Size Distributions in Low-Level Stratiform Clouds. J. Atmos. Sci. 57, 295-311.

Moore, K.F., Sherman, D.E., Reilly, J.E., Hannigan, M.P., Lee, T., Collett, J.L. (2004) Drop size-dependent chemical composition of clouds and fogs. Part II: Relevance to interpreting the aerosol/trace gas/fog system. Atmos. Environ. 38, 1403-1415.

Morales, J.A., Pirela, D., Nava, M.G.D., Borrego, B.Z.S.D., Velásquez, H., Durán, J. (1998) Inorganic water soluble ions in atmospheric particles over Maracaibo Lake Basin in the western region of Venezuela. Atmos. Res. 46, 307-320.

Ogawa, N., Kikuchi, R., Okamura, T., Inotsume, J., Adzuhata, T., Ozeki, T., Kajikawa, M. (2000) Evaluation of ionic pollutants in cloud droplets at a mountain ridge in northern Japan using constrained oblique rotational factor analysis. Atmos. Res. 54, 279-283.

Portin, H., Leskinen, A., Hao, L., Kortelainen, A., Miettinen, P., Jaatinen, A., Laaksonen, A., Lehtinen, K.E.J., Romakkaniemi, S., Komppula, M. (2013) The effect of local sources on particle size and chemical composition and their role in aerosol-cloud interactions at Puijo measurement station. Atmos. Chem. Phys. 13, 32133-32173.

Ravishankara, A.R. (1997) Heterogeneous and Multiphase Chemistry in the Troposphere. Science 276, 1058-1065.

Schell, D., Wobrock, W., Maser, R., Preiss, M., Jaeschke, W., Georgii, H.W., Gallagher, M.W., Bower, K.N., Beswick, K.M., Pahl, S. (1997) The size-dependent chemical composition of cloud droplets. Atmos. Environ. 31, 2561–2576.

Sripa, P., Tongraar, A., Kerdcharoen, T. (1996) Chemical composition of fogwater in an urban area: Strasbourg (France). Environ. Pollut. 94, 345-354.

Sun, M., Wang, Y., Wang, T., Fan, S., Wang, W., Li, P., Guo, J., Li, Y. (2010) Cloud and the corresponding precipitation chemistry in south China: Water‐soluble components and pollution transport. J. Geophys. Res.: Atmos. 115.

Sun, X., Wang, Y., Li, H., Yang, X., Sun, L., Wang, X., Wang, T., Wang, W. (2016) Organic acids in cloud water and rainwater at a mountain site in acid rain areas of South China. Environmental Sci. Pollut. Res. 23, 9529.

Talbot, R.W., Beecher, K.M., Harriss, R.C., Iii, W.R.C. (1988) Atmospheric Geochemistry of Formic and Acetic Acids at a MidLatitude Temperate Site. J. Geophys. Res. Atmos. 93, 1638-1652.

Tan, Y., Carlton, A.G., Seitzinger, S.P., Turpin, B.J. (2010) SOA from methylglyoxal in clouds and wet aerosols: Measurement and prediction of key products. Atmos. Environ. 44, 5218-5226.

Tanner, P.A., Law, P.T. (2003) Organic Acids in the Atmosphere and Bulk Deposition of Hong Kong. Water Air Soil Pollut. 142, 279-297.

Van Pinxteren, D., Fomba, K.W., Mertes, S., Müller, K., Spindler, G., Schneider, J., Lee, T., Collett, J., Herrmann, H. (2015) Cloud water composition during HCCT-2010: Scavenging efficiencies, solute concentrations, and droplet size dependence of inorganic ions and dissolved organic carbon. Atmos. Chem. Phys. 15, 24311-24368.

Wang, X., Ye, X., Chen, H., Chen, J., Yang, X., Gross, D.S. (2014) Online hygroscopicity and chemical measurement of urban aerosol in Shanghai, China. Atmos. Environ. 95, 318-326.

Wang, Y., Guo, J., Wang, T., Ding, A., Gao, J., Yang, Z., Collett, J.L., Wang, W. (2011) Influence of regional pollution and sandstorms on the chemical composition of cloud/fog at the summit of Mt. Taishan in northern China. Atmos. Res. 99, 434-442.

Wang, Y., Wai, K.M., Gao, J., Liu, X., Wang, T., Wang, W. (2008) The impacts of anthropogenic emissions on the precipitation chemistry at an elevated site in North-eastern China. Atmos. Environ. 42, 2959-2970.

Watanabe, K., Honoki, H., Iwai, A., Tomatsu, A., Noritake, K., Miyashita, N., Yamada, K., Yamada, H., Kawamura, H., Aoki, K. (2010) Chemical Characteristics of Fog Water at Mt. Tateyama, Near the Coast of the Japan Sea in Central Japan. Water, Air, Soil Pollut. 211, 379-393.

Xu, P., Liao, Y.J., Lin, Y.H., Zhao, C.X., Yan, C.H., Cao, M.N., Wang, G.S., Luan, S.J. (2015) High-resolution inventory of ammonia emissions from agricultural fertilizer in China from 1978 to 2008. Atmos. Chem. Phys. 15, 25299-25327.

Xu, W., Wang, F., Li, J., Tian, L., Jiang, X., Yang, J., Chen, B. (2017) Historical variation in black carbon deposition and sources to Northern China sediments. Chemosphere 172, 242-248.

Yang, L., Zhou, X., Wang, Z., Zhou, Y., Cheng, S., Xu, P., Gao, X., Nie, W., Wang, X., Wang, W. (2012) Airborne fine particulate pollution in Jinan, China: Concentrations, chemical compositions and influence on visibility impairment. Atmos. Environ. 55, 506-514.

Ye, X., Ma, Z., Hu, D., Yang, X., Chen, J. (2011) Size-resolved hygroscopicity of submicrometer urban aerosols in Shanghai during wintertime. Atmos. Res. 99, 353-364.

Yin, J., Wang, D., Zhai, G. (2011) Long-term in situ measurements of the cloud-precipitation microphysical properties over East Asia. Atmos. Res. 102, 206-217.

Zapletal, M., Kuňák, D., Chroust, P. (2007) Chemical characterization of rain and fog water in the Cervenohorske Sedlo (Hruby Jesenik Mountains, Czech Republic). Water, air, soil pollut. 186, 85-96.

Zimmermann, F., Lux, H., Maenhaut, W., Matschullat, J., Plessow, K., Reuter, F., Wienhaus, O. (2003) A review of air pollution and atmospheric deposition dynamics in southern Saxony, Germany, Central Europe. Atmos. Environ. 37, 671-691.

Zipori, A., Rosenfeld, D., Tirosh, O., Teutsch, N., Erel, Y. (2015) Effects of aerosol sources and chemical compositions on cloud drop sizes and glaciation temperatures. J. Geophys. Res. Atmos. 120.

List of Table and Figure Captions

Table 1.

Species	Units	No. Samples	Min	Max	VWM[b]	Percentage
pH	---	39	3.80	6.93	5.87	---
Electrical Conductivity	$\mu S\ cm^{-1}$	39	44.9	813.5	169.0	---
Na^+	$mg\ L^{-1}$	39	BDL[a]	2.9	0.9	0.56
NH_4^+	$mg\ L^{-1}$	39	5.2	143.3	34.2	21.41
K^+	$mg\ L^{-1}$	39	BDL[a]	6.5	1.3	0.81
Mg^{2+}	$mg\ L^{-1}$	39	0.2	3.0	0.7	0.44
Ca^{2+}	$mg\ L^{-1}$	39	BDL[a]	39.2	5.9	3.69
Cl^-	$mg\ L^{-1}$	39	0.6	11.7	2.9	1.82
NO_3^-	$mg\ L^{-1}$	39	2.7	538.5	56.4	35.31
SO_4^{2-}	$mg\ L^{-1}$	39	10.5	253.0	44.2	27.67
nss-SO_4^{2-}	$mg\ L^{-1}$	39	10.5	251.6	43.7	---
lactate	$mg\ L^{-1}$	13	BDL[a]	7.8	3.0	1.88
acetate	$mg\ L^{-1}$	15	BDL[a]	14.9	4.1	2.57
formate	$mg\ L^{-1}$	17	0.4	14.4	2.8	1.75
oxalate	$mg\ L^{-1}$	17	0.6	3.6	1.3	0.81
Mn	$mg\ L^{-1}$	39	0.01	0.28	0.04	0.03
Fe	$mg\ L^{-1}$	39	0.06	3.02	0.40	0.25
HCHO	$mg\ L^{-1}$	39	BDL[a]	5.9	0.4	0.25
H_2O_2	$mg\ L^{-1}$	39	BDL[a]	3.3	0.8	0.50
S(IV)	$mg\ L^{-1}$	39	BDL[a]	1.1	0.4	0.25
OC[c]	$mg\ L^{-1}$	17	BDL[a]	211.8	37.4	---
EC[d]	$mg\ L^{-1}$	17	BDL[a]	8.5	0.3	---
Average $PM_{2.5}$ Level	$\mu g\ m^{-3}$	39	0.7	81.6	15.9	---

[a] BDL means Below Detection Limit
[b] Volume Weighted Mean Concentration
[c] OC means Organic Carbon
[d] EC means Element Carbon

Table 2.

Site	Period	Altitude (m)	pH	EC ($\mu S\ cm^{-1}$)	Na^+	NH_4^+	K^+	Mg^{2+}	Ca^{2+}	Cl^-	NO_3^-	SO_4^{2-}	Reference
Whiteface Mountain, NY USA	May-Sept 2006	1483	3.88	79.6	3.7	149.3	2.1	7.4	26.6	7.2	79.2	220.4	(Aleksic et al., 2009)
Szrenica, Poland	Dec 2005-Dec 2006	1330	4.55	80	100	210	45	49	140	93	240	200	(Błaś et al., 2010)
Mt. Niesen, Swizerland	2006-2007	2362	6.4	34.4	43	143.5	5	12.6	46.8	10.6	87	72.3	(Michna et al., 2015)
Sinhagad, India	2007-2010	1450	6	86	204	28	17	17	196	234	68	198	(Budhavant et al., 2014)
Mt. Heng, China	Mar-May 2009	1279	3.8	115.26	66.03	356.47	17.25	5.49	29.83	21.07	158.8	196.39	(Sun et al., 2010)
Mt. Tai, China	2007-2008	1545	3.86	---	25.0	1215	55.1	33.0	193	93.4	407	1064	(Guo et al., 2012)
Mt. Tai, China This Work	Jul-Oct 2014	1545	5.87	169.0	39.7	1900.8	32.7	60.5	295.5	82.5	910.2	920.9	

Table 3.

Event Number	Start (UTC/GMT+8)	Stop (UTC/GMT+8)	No. Samples	Duration (h)	[a]$PM_{2.5}$ ($\mu g\ m^{-3}$)	[a]LWC ($g\ m^{-3}$)	[a]N_d ($\#\ cm^{-3}$)	[a]MVD (μm)	[a]ED (μm)	T (℃)	[a]RH (%)
1	24/07/2014 08:30	24/07/2014 23:20	3	14.8	14.5	0.24	408	12.7	11.0	15.5-22.6	97.9
2	[b]25/07/2014 12:00	25/07/2014 21:40	2	9.7	11.1	0.18	719	8.3	8.3	13.6-14.6	100.0
3	26/07/2014 23:06	27/07/2014 05:13	0	6.1	100.7	0.04	211	7.8	7.4	15.7-17.0	99.0
4	[b]28/07/2014 22:40	29/07/2014 04:00	1	5.3	81.6	0.09	337	8.2	7.8	16.5-17.6	99.2
5	29/07/2014 20:33	29/07/2014 22:20	0	1.8	65.6	0.14	694	7.8	7.6	18.5-18.9	99.3
6	30/07/2014 12:46	30/07/2014 13:50	1	1.1	13.2	0.21	308	12.6	11.8	16.8-18.5	99.5
7	[b]30/07/2014 20:20	30/07/2014 22:40	0	2.3	25.0	0.08	253	9.2	9.2	16.9-18.2	99.6
8	31/07/2014 19:11	01/08/2014 09:19	2	14.1	20.1	0.18	329	12.6	11.5	17.9-19.1	99.5
9	04/08/2014 23:42	05/08/2014 11:30	1	11.8	65.8	0.13	539	9.0	8.5	19.5-21.9	99.3
10	05/08/2014 18:45	06/08/2014 06:13	1	11.5	40.0	0.11	227	11.1	9.8	16.0-20.3	99.3
11	09/08/2014 07:41	09/08/2014 09:32	0	1.8	17.4	0.06	261	7.9	7.7	13.7-14.0	100.0
12	11/08/2014 20:42	11/08/2014 21:09	0	0.4	173.3	0.06	392	8.3	7.7	17.6-17.9	99.7
13	12/08/2014 23:04	13/08/2014 03:55	2	4.8	66.1	0.19	536	9.4	9.1	13.8-16.9	99.0
14	13/08/2014 18:58	14/08/2014 06:22	3	11.4	34.5	0.19	312	10.9	9.7	13.5-15.9	98.4
15	14/08/2014 17:35	14/08/2014 19:52	0	2.3	94.6	0.02	104	7.2	6.5	15.7-17.7	98.8
16	15/08/2014 18:52	16/08/2014 05:59	0	11.1	66.4	0.04	283	6.9	6.5	15.0-17.6	99.2
17	16/08/2014 19:45	17/08/2014 05:10	0	9.4	93.9	0.03	157	8.3	7.3	15.5-18.2	98.4
18	17/08/2014 10:02	17/08/2014 11:13	1	1.2	63.5	0.39	722	11.7	10.6	14.9-17.0	99.2
19	17/08/2014 21:57	18/08/2014 01:23	1	3.4	52.5	0.10	366	8.5	8.3	14.3-15.2	99.1
20	18/08/2014 08:42	18/08/2014 11:05	0	2.4	---	0.03	118	7.2	6.8	15.0-16.5	98.4
21	21/08/2014 20:00	22/08/2014 13:48	0	17.8	57.9	0.02	109	7.0	6.5	15.9-20.7	96.3
22	[b]23/08/2014 01:30	23/08/2014 09:20	3	7.8	43.0	0.21	624	9.6	9.4	16.2-17.4	99.6
23	23/08/2014 18:12	23/08/2014 19:54	0	1.7	70.6	0.01	88	6.8	6.3	16.8-17.8	99.5
24	25/08/2014 02:25	25/08/2014 06:40	0	4.2	29.4	0.01	79	5.7	5.3	13.8-15.0	97.8

[a] the arithmetic mean value

[b] the selected four typical cloud events according to the average $PM_{2.5}$ level for 28/07/2014 22:40 to 29/07/2014 04:00 (event A, 81.6 $\mu g\ m^{-3}$), 23/08/2014 01:30 to 23/08/2014 09:20 (event B, 43.0 $\mu g\ m^{-3}$), 30/07/2014 20:20 to 30/07/2014 22:40 (event C, 25.0 $\mu g\ m^{-3}$) and 25/07/2014 12:00 to 25/07/2014 21:40 (event D, 11.1 $\mu g\ m^{-3}$).

Figure 1:

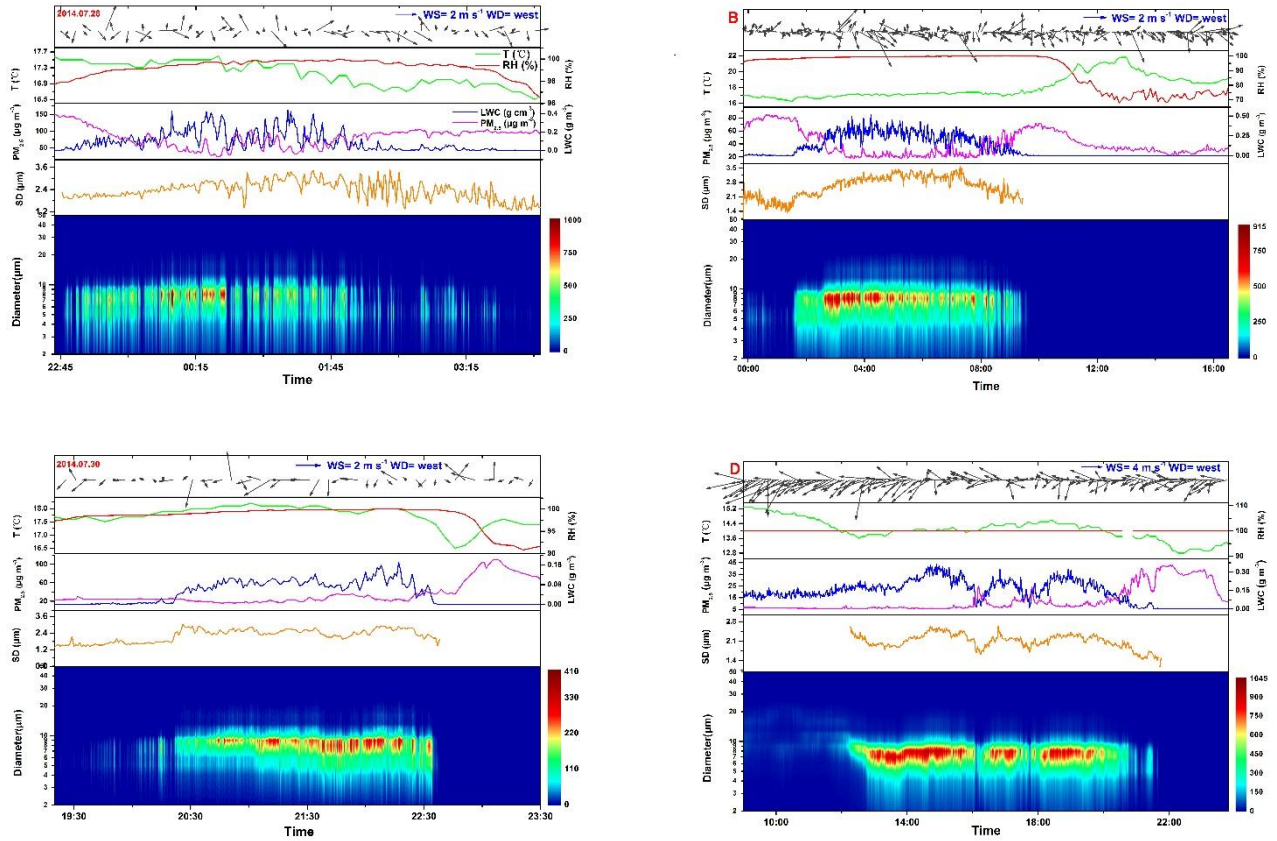
2014.07.28
WS= 2 m s-1 WD= west
T (℃)
RH (%)
LWC (g cm-3)
PM2.5 (μg m-3)
SD (μm)
Diameter(μm)
Time
B
WS= 2 m s-1 WD= west
Time
2014.07.30
WS= 2 m s-1 WD= west
Time
D
WS= 4 m s-1 WD= west
Time

Figure 2:

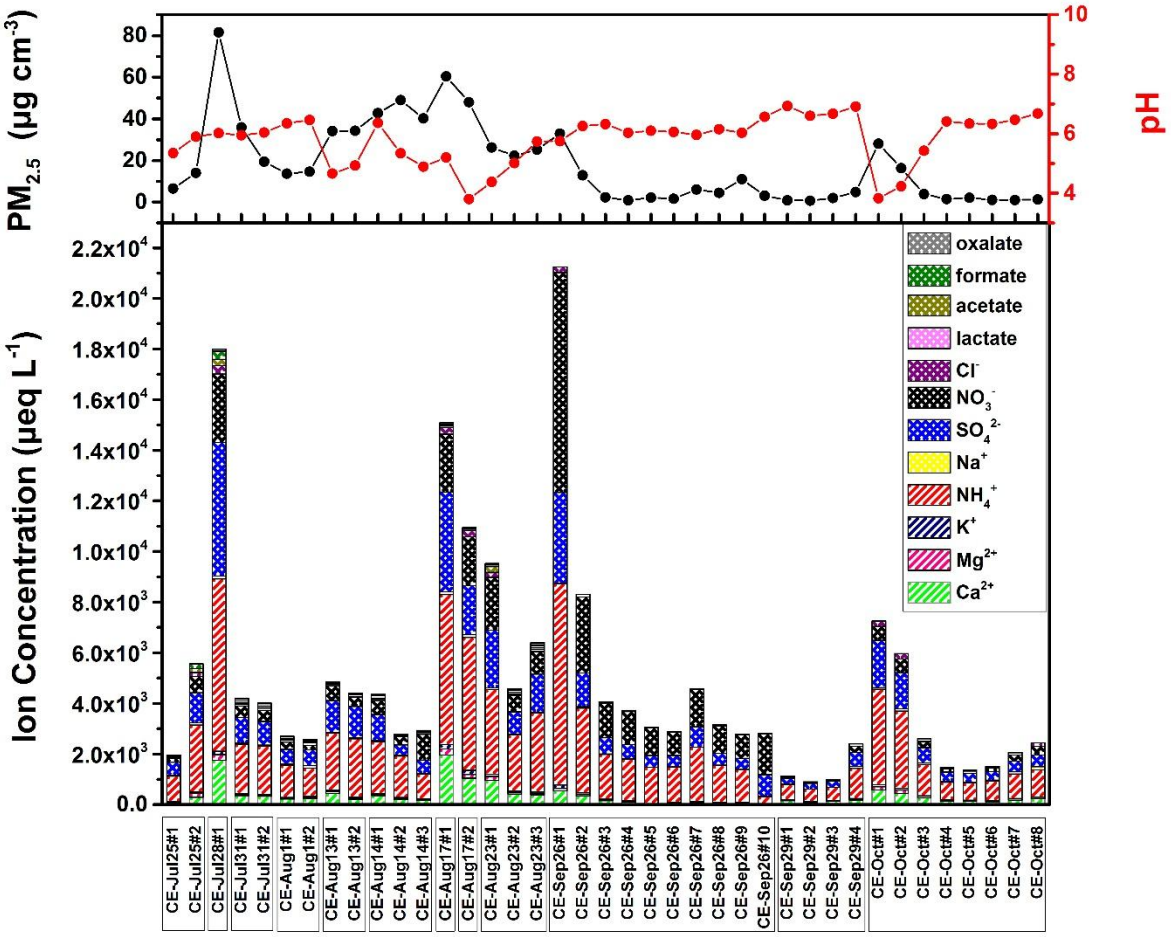
PM2.5 (μg cm-3)
pH
Ion Concentration (μeq L-1)
oxalate
formate
acetate
lactate
Cl-
NO3-
SO4 2-
Na+
NH4+
K+
Mg2+
Ca2+
CE-Jul25#1
CE-Jul25#2
CE-Jul28#1
CE-Jul31#1
CE-Jul31#2
CE-Aug1#1
CE-Aug1#2
CE-Aug13#1
CE-Aug13#2
CE-Aug14#1
CE-Aug14#2
CE-Aug14#3
CE-Aug17#1
CE-Aug17#2
CE-Aug23#1
CE-Aug23#2
CE-Aug23#3
CE-Sep26#1
CE-Sep26#2
CE-Sep26#3
CE-Sep26#4
CE-Sep26#5
CE-Sep26#6
CE-Sep26#7
CE-Sep26#8
CE-Sep26#9
CE-Sep26#10
CE-Sep29#1
CE-Sep29#2
CE-Sep29#3
CE-Sep29#4
CE-Oct#1
CE-Oct#2
CE-Oct#3
CE-Oct#4
CE-Oct#5
CE-Oct#6
CE-Oct#7
CE-Oct#8

Figure 3:

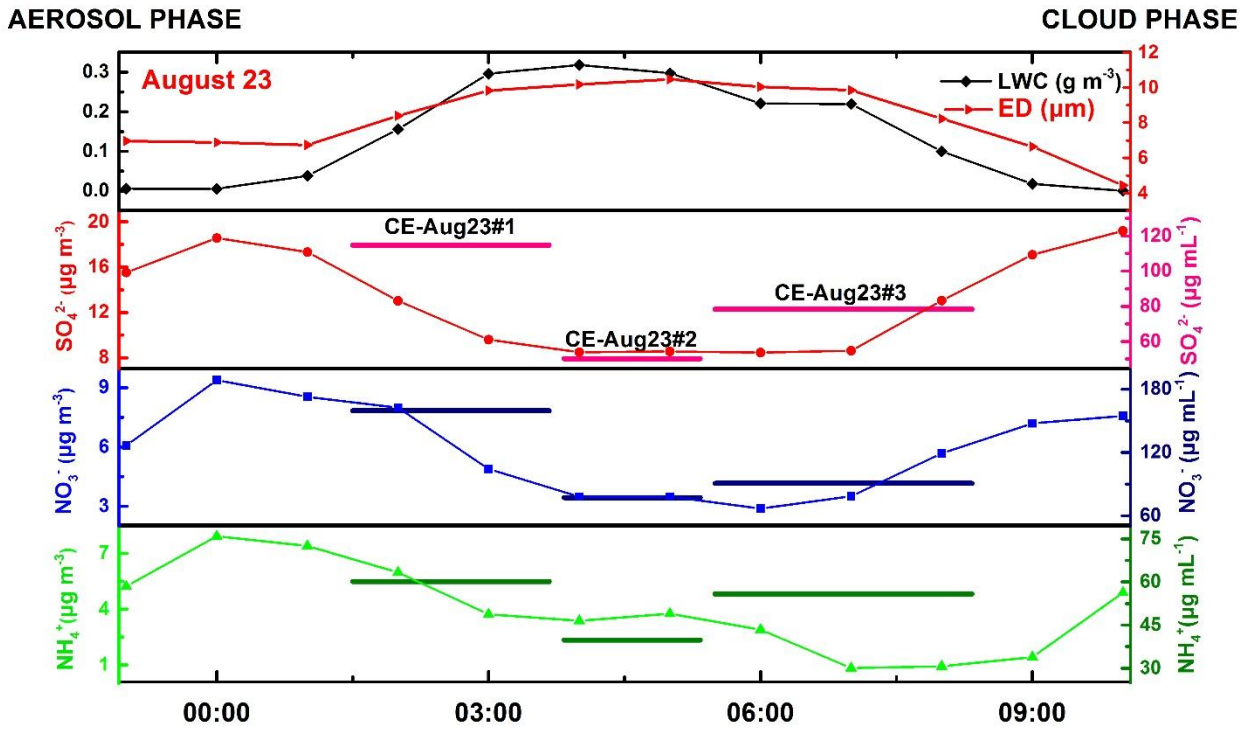
AEROSOL PHASE
CLOUD PHASE
August 23
LWC (g m-3)
ED (μm)
CE-Aug23#1
CE-Aug23#2
CE-Aug23#3
SO4 2- (μg m-3)
SO4 2- (μg mL-1)
NO3 - (μg m-3)
NO3 - (μg mL-1)
NH4 + (μg m-3)
NH4 + (μg mL-1)
00:00
03:00
06:00
09:00

Figure 4:

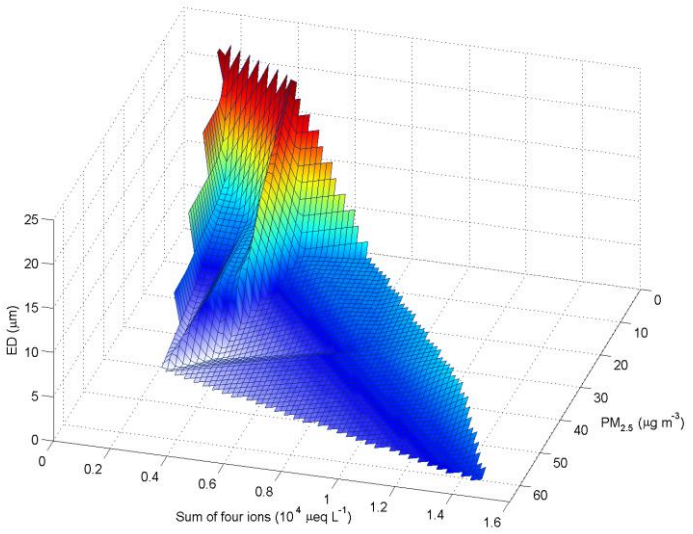
ED (μm)
0
5
10
15
20
25
0
0.2
0.4
0.6
0.8
1
1.2
1.4
1.6
Sum of four ions (10^4 μeq L^-1)
0
10
20
30
40
50
60
PM2.5 (μg m^-3)

(a)

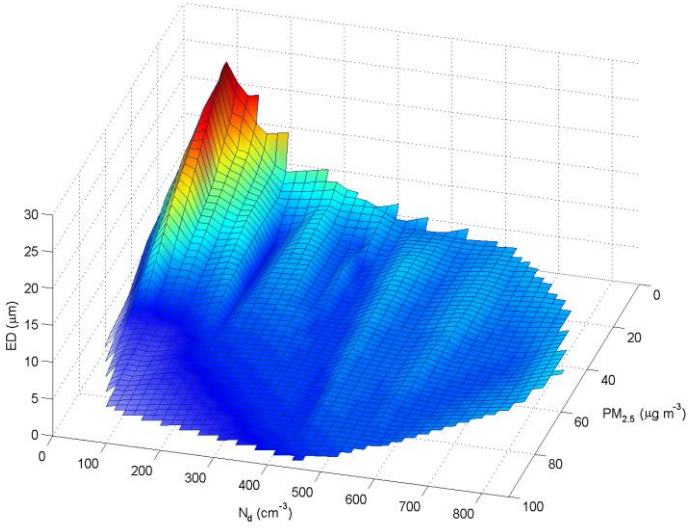
ED (μm)
0
5
10
15
20
25
30
0
100
200
300
400
500
600
700
800
Nd (cm^-3)
0
20
40
60
80
100
PM2.5 (μg m^-3)

(b)

Figure 5:

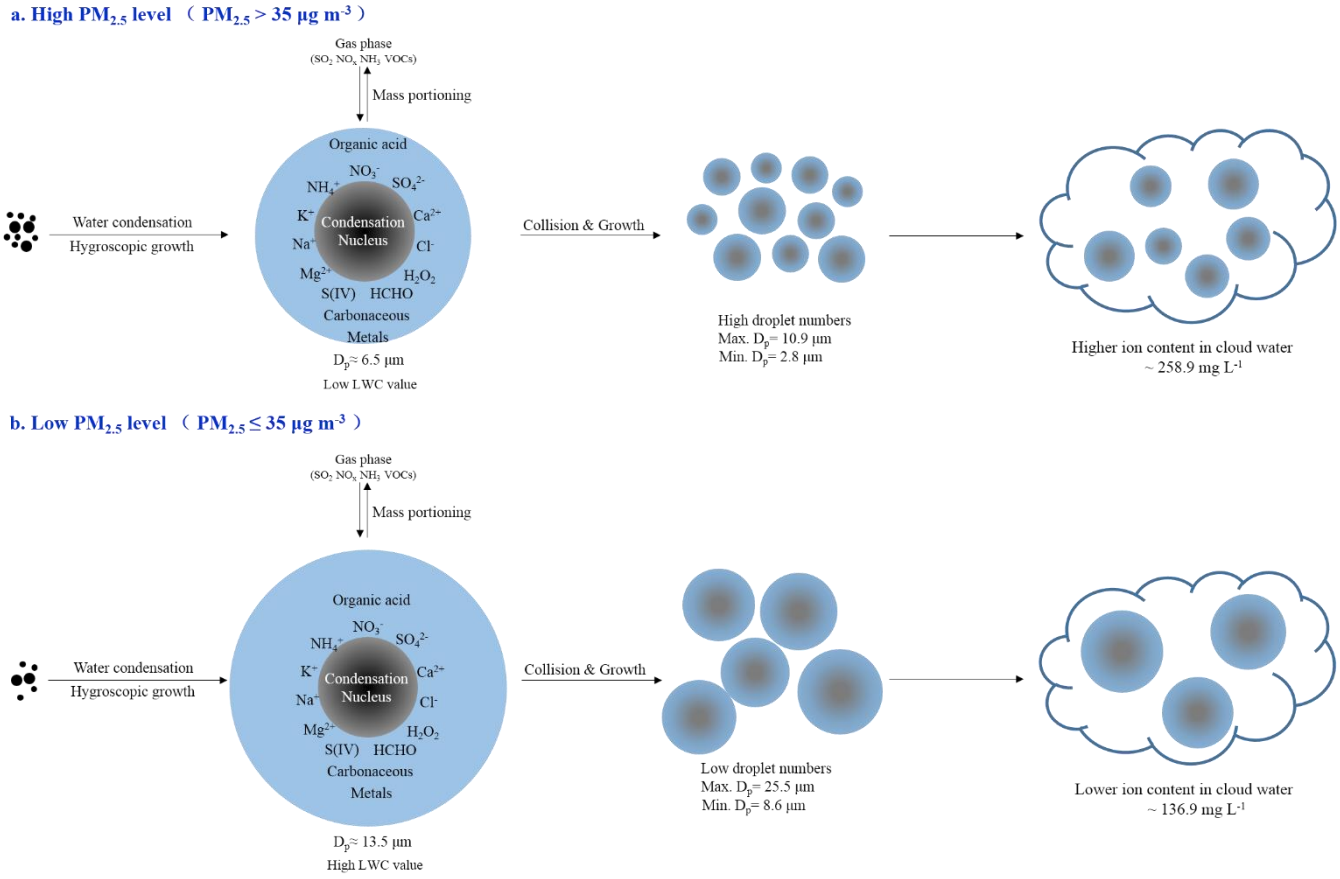
a. High $PM_{2.5}$ level （ $PM_{2.5}$ > 35 μg m^{-3} ）
Gas phase
(SO_2 NO_x NH_3 VOCs)
Mass portioning
Organic acid
NO_3^-
NH_4^+
SO_4^{2-}
K^+
Ca^{2+}
Condensation Nucleus
Na^+
Cl^-
Mg^{2+}
H_2O_2
S(IV) HCHO
Carbonaceous
Metals
Water condensation
Hygroscopic growth
D_p≈ 6.5 μm
Low LWC value
Collision & Growth
High droplet numbers
Max. D_p= 10.9 μm
Min. D_p= 2.8 μm
Higher ion content in cloud water
~ 258.9 mg L^{-1}
b. Low $PM_{2.5}$ level （ $PM_{2.5}$ ≤ 35 μg m^{-3} ）
Gas phase
(SO_2 NO_x NH_3 VOCs)
Mass portioning
Organic acid
NO_3^-
NH_4^+
SO_4^{2-}
K^+
Ca^{2+}
Condensation Nucleus
Na^+
Cl^-
Mg^{2+}
H_2O_2
S(IV) HCHO
Carbonaceous
Metals
Water condensation
Hygroscopic growth
D_p≈ 13.5 μm
High LWC value
Collision & Growth
Low droplet numbers
Max. D_p= 25.5 μm
Min. D_p= 8.6 μm
Lower ion content in cloud water
~ 136.9 mg L^{-1}